

Article

Multimodal Power Management Based on Decision Tree for Internet of Wearable Things Systems

Jaime Ortegón-Aguilar ¹, Alejandro Castillo-Atoche ², Guillermo Becerra-Nuñez ¹,
Johan Jair Estrada-López ³, Edith Osorio-de-la-Rosa ¹, Roberto Carrasco-Alvarez ⁴, Asim Datta ⁵
and Javier Vázquez-Castillo ^{1,*}

¹ Informatics and Networking Department, Universidad Autónoma del Estado de Quintana Roo, Chetumal 77019, Mexico

² Robotics and Industry 4.0 Laboratory, Mechatronics Department, Autonomous University of Yucatan, Mérida 97000, Mexico

³ Faculty of Mathematics, Autonomous University of Yucatan, Mérida 97000, Mexico

⁴ Electro-Fotonics Department, CUCEI-Guadalajara University, Blvd. Marcelino García Barragán 1421, Guadalajara 44430, Mexico

⁵ Department of Electrical Engineering, Tezpur University, Tezpur 784028, Assam, India

* Correspondence: jvazquez@uqroo.edu.mx

Abstract: Precision medicine is now evolving to include internet-of-wearable-things (IoWT) applications. This trend requires the development of novel systems and digital signal processing algorithms to process large amounts of data in real time. However, performing continuous measurements and complex computational algorithms in IoWT systems demands more power consumption. A novel solution to this problem consists in developing energy-aware techniques based on low-power machine learning (ML) algorithms to efficiently manage energy consumption. This paper proposes a multimodal dynamic power management strategy (DPMS) based on the ML-decision tree algorithm to implement an autonomous IoWT system. The multimodal approach analyzes the supercapacitor storage level and the incoming biosignal statistics to efficiently manage the energy of the wearable device. A photoplethysmography (PPG) sensing prototype was developed to evaluate the proposed ML-DPMS programmed in a Nordic nRF52840 processor. The experimental results demonstrate an IoWT system's low consumption of 25.74 J, and a photovoltaic solar power generation capacity of 380 mW. The proposed ML-DPMS demonstrates a battery life extension of $3.87 \times$, i.e., 99.72 J of energy harvested, which represents the possibility to achieve at least $2.4 \times$ more data transmissions, in comparison with the widely used uniform power management approach. In addition, when the supercapacitor's energy is compromised, the decision tree technique achieves a good energy conservation balance consuming in the same period of time 39.6% less energy than the uniform power approach.

Keywords: internet of wearable things; machine learning; power management; wireless sensor networks



Citation: Ortegón-Aguilar, J.; Castillo-Atoche, A.; Becerra-Nuñez, G.; Estrada-López, J.J.; Osorio-de-la-Rosa, E.; Carrasco-Alvarez, R.; Datta, A.; Vázquez-Castillo, J. Multimodal Power Management Based on Decision Tree for Internet of Wearable Things Systems. *Appl. Sci.* **2023**, *13*, 4351. <https://doi.org/10.3390/app13074351>

Academic Editor: Juan Francisco De Paz Santana

Received: 30 January 2023

Revised: 23 March 2023

Accepted: 27 March 2023

Published: 29 March 2023



Copyright: © 2023 by the authors. Licensee MDPI, Basel, Switzerland. This article is an open access article distributed under the terms and conditions of the Creative Commons Attribution (CC BY) license (<https://creativecommons.org/licenses/by/4.0/>).

1. Introduction

Wearable and artificial intelligence (AI) technologies play an increasingly important role in modern medical fields by enabling remote diagnostics and monitoring of health conditions [1–6]. Recent studies on precision medicine measure biological signals (heart rate, body temperature, blood oxygen saturation) for the smart detection and monitoring of diseases and physical disorders [7–14]. However, the need for continuous measurements, analysis, and transmission in novel wearable systems requires more computational power, resulting in higher energy consumption. Internet-of-wearable-things (IoWT) devices are commonly battery-powered; therefore, one key design problem is enhancing the energy efficiency of IoWT systems [15,16]. In this sense, the wearable end device does not have

to measure and transmit data continuously. Instead, it can go to sleep for long periods of time and periodically wake up to sample the biological signs. Once a sensitive event is detected, the sensor can then stay active to acquire more data and transmit it to the cloud. This event-driven pattern is accurate and may not miss any event occurrences, as long as the wake-up period is short enough. However, when the system operates in this mode, its energy consumption increases and fluctuates randomly, making it hard to predict if enough energy is preserved in the storage system for the device to wake up and sense cyclically.

In the past, diverse dynamic power management strategies (DPMS) and energy harvesting approaches have been proposed to enhance the energy efficiency of wearable healthcare devices [6,16–19]. In [20–22], DPMS reduced the energy consumption of healthcare devices, identifying the duration and timing of sleep cycling. Moreover, [23] recommends artificial neural networks (ANN) to estimate DPMS wake-up schedules to save energy. Task offloading is another energy-efficiency perspective to reduce the power consumption on wearable devices [24]. However, these strategies rely on cloud services for complex computational operations, which depend on stable internet connectivity [25].

Decision tree (DT) algorithms are a subset of machine learning (ML) that can be used for implementing low-cost hardware implementations [26]. This is because DT uses logical comparators only, which are efficiently synthesized by compilation libraries. On the other hand, neural networks (or classical embedded implementation [27]) and other approaches perform arithmetic operations such as additions, multiplications, or even more complex operations depending on the activation function. For example, [28] discusses the computational complexity of hardware implementations of decision trees and their usage in data classification. The hardware implementation of DT with 8 trees depth requires $257 \times$ fewer MAC (multiply–accumulate) operations compared to an 8-layer CNN and $43 \times$ fewer MAC operations compared to a 5-layer CNN. This reduction in MAC operations results in a lower area and power consumption implementation [28].

In this paper, a multimodal power management strategy is proposed for intelligent energy use in IoWT systems. A decision tree algorithm based on machine learning (ML) is efficiently implemented as a strategy to maximize the number of transmissions, considering the limited and time-varying amount of available energy, and minimize the energy consumption if the incoming data does not show the occurrence of a sensitive event. The ML-DPMS is programmed in the Nordic nRF52840 microcontroller unit (MCU) maintaining a low-power approach.

Figure 1 illustrates the conceptual idea of the proposed IoWT system. As can be seen, a PPG (photoplethysmography)-based IoWT system prototype is developed to experimentally evaluate the multimodal power management operation with the ML-decision tree algorithm. The system integrates an energy harvesting (EH) circuit and the MCU with a Bluetooth low energy (BLE) module built into the same device. The main contributions of this paper are the following:

- A multimodal ML-DPMS approach that increases by at least $2.4 \times$ the number of transmissions in comparison to uniform power management approaches when the incoming biosignal data has high variability, and the power of the supercapacitor is sufficient and achieves a good energy saving of up to 39.6%, avoiding system shutdown, when the supercapacitor's energy is low.
- A low consumption of 25.72 J for the IoWT system based on the ML-decision tree algorithm programmed in the Nordic nRF52840 MCU. A 380.8 mW solar PV (photovoltaic) power generation system (i.e., 99.7 J of energy harvested per day) which is 3.87 times more than the energy required for operation.
- A highly integrated PPG-based wearable prototype to evaluate the ML-decision tree power management strategy.

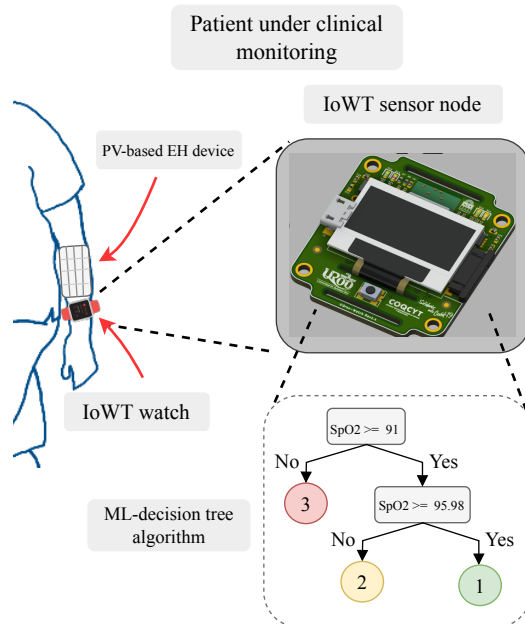


Figure 1. Conceptual idea of the proposed wearable IoT sensor node, which implements ML-based dynamic power management strategies.

The remainder of this study is organized as follows: Section 2 presents the developed PPG-based IoWT sensor node prototype with the solar PV EH circuit. Section 3 describes the multimodal intelligent energy DPMS. Experimental results on real-time embedded hardware implemented on the wearable platform are presented in Section 5. Finally, the conclusions are stated in Section 6.

2. Circuit Design of the PPG-Based Wearable System

A highly integrated IoWT system prototype was designed to evaluate the proposed power management strategy. Figure 2 shows a system-level diagram of the proposed circuit prototype.

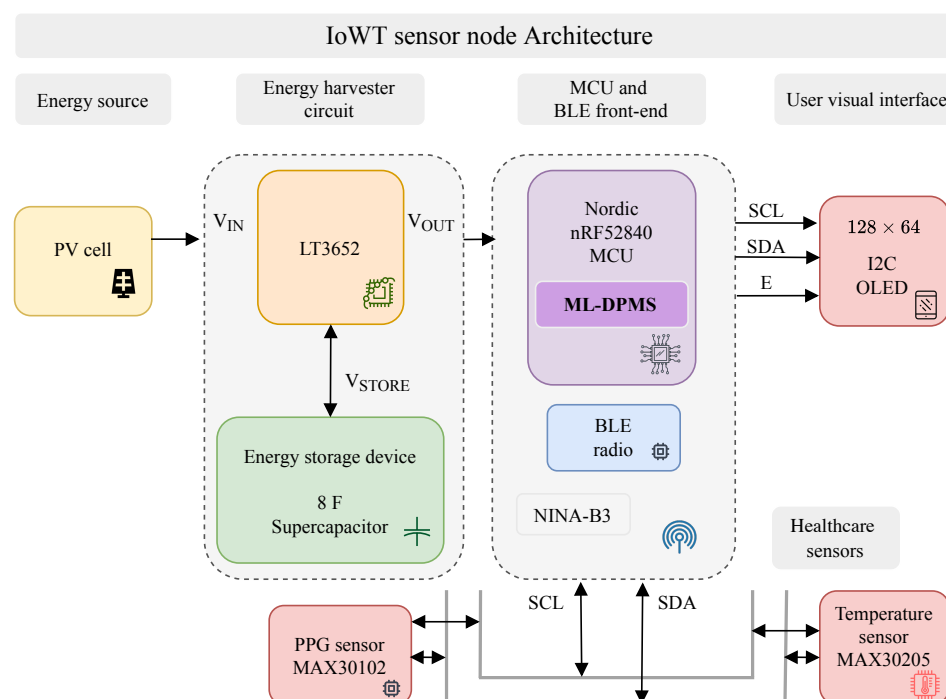


Figure 2. Schematic diagram of the proposed PPG-based sensing system.

2.1. Energy Harvesting Circuit

The EH circuit is connected to a small 80×100 mm, 1 W solar PV cell, with a typical energy transformation efficiency of 35% [29]. The mono-crystalline panel has an open circuit voltage of 8.2 V, with a voltage and current at the maximum power point of 6.4 V and 170 mA, respectively. The EH circuit is based on the LT3652 (Analog Device, Wilmington, MA, USA) monolithic step-down converter that operates with a minimum input voltage of 4.95 V. It is compatible with low-power systems, i.e., once charging is terminated, it enters standby mode with a low-power consumption of 85 μ A. The LT3652 maximizes the transfer of energy from the PV panel to an 8 F supercapacitor array, with an energy capacity of 54.76 J for the IoT system operation. The LT3652 uses a charge-current scheme, which ends a charge cycle when the supercapacitor charge current falls to one-tenth of the programmed 1.0 A maximum charge current. On the other hand, when the supercapacitor voltage reaches 60% of the fully charged float voltage, the IC automatically increases the maximum charge current to the full programmed value. Once charging is terminated, the LT3652 automatically enters a low-current standby mode where supply bias currents are reduced to 85 μ A.

2.2. Microcontroller Unit with BLE Wireless Communication

The NINA-B302 (U-Blox, Thalwil, CH) module integrates a small, stand-alone Bluetooth low energy (BLE)-5 circuit with the nRF52840 MCU (Nordic Semiconductors, Trondheim, NO, Norway) [30]. It also encloses a planar inverted-F antenna, that is successfully tuned with a passive network of inductor and capacitor components, producing a well-matched transceiver system. The nRF52840 MCU encloses an Arm Cortex-M4, 1 MB flash, and 256 kB RAM. It also contains a CryptoCell CC310 (Nordic Semiconductors, Trondheim, NO, Norway) cryptographic security unit and a high-speed SPI interface at 32 MHz. This chip has a 1.7 to 5.5 V supply voltage range and current consumption of 0.6 μ A in sleep mode and 4.8 mA TX at 0 dBm. The ML-DPMS algorithm is implemented in the MCU and dynamically runs after data acquisition, analyzing the healthcare signs and the supercapacitor level, and adjusting the next IoT's sleep period.

BLE is a wireless communication technology designed for low power consumption and a data rate of up to 2 Mbps. The BLE protocol data unit (PDU) is configured with a packet structure that contains a header and a payload. The PDU is assembled with a preamble, the access address, and the cyclic redundant code (CRC). Figure 3 illustrates the used packet structure of 20 bytes size for BLE transmission that is able to transmit 10 bytes of data per packet, with the possibility to transmit multiple packets in succession.

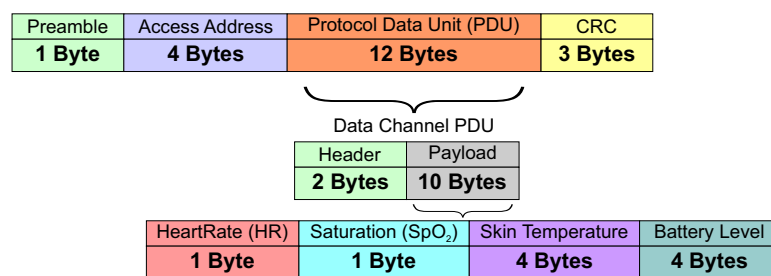


Figure 3. BLE data packet configuration.

2.3. Healthcare Sensors

The MAX30205 (temperature) and the MAX30102 (PPG) sensors from Maxim Integrated (San Jose, CA, USA) [31] are the high-accuracy healthcare components used in the prototype. In particular, the PPG sensor has an embedded processor, which computes advanced R-wave detection algorithms. Despite this processing, the consumption of this sensor is 600 μ A and 0.7 μ A in sleep mode. The I²C interface is used to communicate data from the sensors to the nRF52840 microcontroller host. Figure 4 illustrates the sensors and electronic components assembled in the wearable printed circuit board (PCB) prototype.

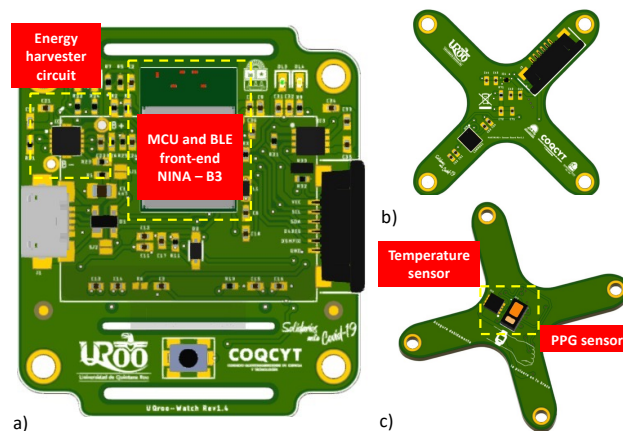


Figure 4. Schematic diagram of the proposed PPG-based prototype. (a) main board top view, (b) sensors' board top view and (c) sensors' board bottom view.

2.3.1. Temperature Sensor

The MAX30205 is a clinical-grade temperature sensor with 16-bit resolution, ± 0.1 °C accuracy, 0 to $+50$ °C operation range, and 2.7 V to 3.3 V supply voltage range. The sensor consumes 600 μ A in typical operating supply current and 1.65 μ A when the sensor is in sleep mode (with the I²C bus inactive). This sensor accomplishes the ASTM E1112 standard specification for an electronic digital thermometer.

2.3.2. Heart Rate and SpO₂-PPG Sensor

The clinical-degree MAX30102 sensor contains a pulse oximetry and a heart rate (HR) module. The sensor comprises internal LEDs, photo-detectors, optical elements, and low-noise electronics with ambient light rejection. It has an integrated cover glass for optimal, robust performance. This sensor is shut down through software (0.7 μ A Typical), allowing a low-power operation with high sample rates and high signal-to-noise-ratio (SNR).

3. Intelligent Power Management

This section describes the multimodal dynamic power management strategy. In particular, machine learning (ML) policies are proposed for power management taking into account the available energy stored in the supercapacitor for the IoWT system and the sensors' data statistics.

A processing chain methodology is presented for analyzing the biosignal statistics and supercapacitor voltage level to efficiently manage the energy of IoWT devices. As illustrated in Figure 5, the variables are intelligently processed by the ML-decision tree to estimate the next sleep period before BLE transmission.

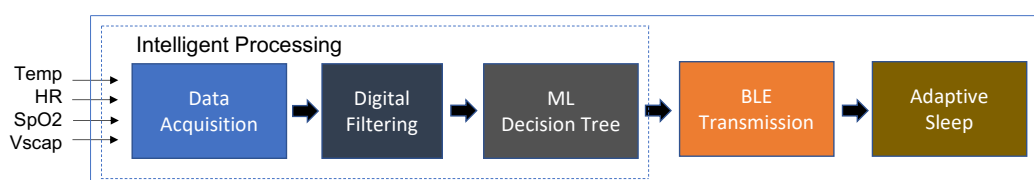


Figure 5. Flowchart diagram of the DPM strategy.

3.1. Data Acquisition

The data acquisition steps and the DPMS strategy are the following:

- Each sampling cycle has $N = 512$ measurements of Temp, SpO₂, and HR. The measurement period takes 20.48 s at a sampling frequency of 25 Hz.
- The supercapacitor's voltage level V_{scap} is also acquired every time the MCU wakes up (T_{Sleep}).

- The moving average algorithm (MA) is implemented in the nRF52840 MCU. That is: $\delta_i = \frac{1}{N}(x_{i,1} + x_{i-1,1} + \dots + x_{i-N,1}; x_{i,2} + x_{i-1,2} + \dots + x_{i-N,2}; x_{i,3} + x_{i-1,3} + \dots + x_{i-N,3})$. The N value is a power of 2, which means that the division is computed by a simple shift operation.
- ML-decision tree processing
- Data transmission δ_i with the BLE protocol
- Sleep period of $T_{sleep} = 15$ min (default value) for IoWT sensing update.

Recent studies have aimed to determine the minimal sampling frequency for PPG signals. One option is optimizing the signal sampling rate by decimating with a factor of 2, 5, 10, 20, 50, 100, 200, 500, then cubic spline and parabola interpolating back to 1 ms resolution [32,33]. However, a 5 Hz sampling frequency is sufficient for the PPG signal's average monitoring. The interpolation method is used to improve the resolution from lower sampling frequencies [32]. In this work, the frequency of 25 Hz is selected for the PPG-based IoWT system. Finally, Elgendi et al. [34] suggest taking three measurements per hour to assess disease conditions using photoplethysmography, with each measurement taking 20 min. In this study, a period ranging from 5 to 15 min was considered to achieve a balance between accuracy and energy savings.

3.2. ML-Decision Tree

Machine learning (ML) is an attractive method for the intelligent management of energy utilization in IoWT systems. Different ML approaches can be used, such as genetic algorithms and neural networks, among others. As Taghavi and Shoaran [28] pointed out, ML-decision trees can be designed with low computational overhead, as they rely on recursive data partitions of the dataset by comparing features with a threshold. This proposal suggests using a low-power decision tree algorithm to efficiently manage energy consumption. ML-decision trees perform simple evaluations (comparisons) on the available features to form homogeneous subsets based on decision rules. Each level of the tree represents a refinement of the subset that guides to a final decision, in this case, the sleep period. The fit algorithm computes decision rules to split the dataset (features and corresponding threshold) once the decision tree is trained. As a result, in the proposed model, an ensemble of four trees (one for each feature) with a depth of k (i.e., $2k - 1$ nodes), the total number of operations required for inference is $4 \times k$ plus the decision.

In this proposal, the multimodal ML-based decision tree estimates the duration of the sensor node's sleep period \hat{T}_{Sleep} according to the data acquisition statistics (Temp, HR, SpO₂), and supercapacitor voltage level (V_{scap}).

ML policies are implemented on the power management approach providing better insight and understanding of the discrete actions taken by the PPG-based IoWT system. The policies follow the National Early Warning System (NEWS) [35], and the control flow is addressed by the Decision tree algorithm to maximize the number of transmitted packets considering the level of available energy.

A state vector $\zeta_i = (T_i, SpO2_i, HR_i, V_{scap}, T_{sleep})$ is established describing the state of the PPG-based IoWT system. In this regard, for every measurement of the variables, the ML algorithm establishes the split actions following the NEWS statements and estimates the best \hat{T}_{sleep} period. The decision tree algorithm selects the weights associated with each ζ_i , and the thresholds β_{Th} .

The algorithm comprises three main steps:

- The initial information entropy of the sample set $H(\zeta)$ is calculated as

$$H(\zeta) = - \sum_{i=1}^m p_i \log_2 p_i. \quad (1)$$

where ζ is the sample set, p_i represents the probability of samples, and m is the number of classes, which matches the sleep system periods.

- The split entropy of the sample set under a selected action is calculated assuming that ζ is divided into two subsets $\{\zeta_L, \zeta_R\}$ by a randomly selected action A . The split entropy is shown as follows:

$$H_A(\zeta) = \frac{|\zeta_L|}{|\zeta|} H(\zeta_L) + \frac{|\zeta_R|}{|\zeta|} H(\zeta_R). \quad (2)$$

- The information gain is computed by subtracting (2) from (1),

$$Gain(A) = H(\zeta) - H_A(\zeta) \quad (3)$$

Finally, the decision tree algorithm is trained to fit the state-action data through supervised learning using Matlab's statistics and machine learning toolbox. An amount of 4000 samples of HR, Temp, SpO₂, and Vscap were used for training based on the NEWS standard. Data were divided into training and test sets.

4. Experimental Results

The wearable prototype performs on-body monitoring testing, and an Android application visualizes the data online. Google's toolkit, Flutter, and Amazon web service (AWS) were used for data storage and remote diagnosis through the website. The BLE transceiver was configured for 0 dB power transmission, which is enough for a range cover of 10 to 15 m.

Figure 6 depicts the experiment results of the IoWT prototype. Figure 6a, shows the wearable electronic system prototype. Figure 6b illustrates a classification example result with a splitting tree diagram for data analysis. The state variable HR is split through the tree reaching the respective action A_K according to the NEWS statement, i.e., $\{A_K: \text{circle green, circle yellow, circle red}; K = 1, 2, 3\}$. The weights were calculated offline through the training process.

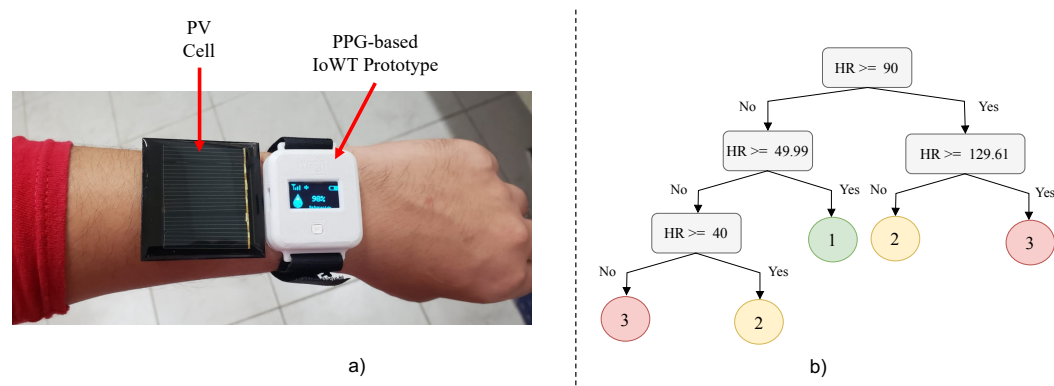


Figure 6. Experimental results: (a) Wearable electronic prototype with decision tree power management; and (b) Decision tree split result example.

4.1. Power Consumption and Energy Harvester Analysis

Figure 7 shows the supercapacitor's voltage recovery after one transmission cycle. After BLE pairing, the system enters an active sensing state performing the 512 measurements in 20.48 s. It is observed that the BLE transmission causes a 100 mV voltage drop; however, the supercapacitor recovery is almost instantaneous when the system achieves sleep mode. The processing state corresponds to the ML-decision tree algorithm implemented on the MCU, which estimates the next sleep period \hat{T}_{sleep} .

The supercapacitor charging test shows a quick charge recovery in a few seconds (≈ 2 s). This suggests what could be considered the minimum sleep period to allow for the supercapacitor charging. However, other factors, such as temperature and solar radiation, must also be considered. In this study, the power management analysis based on the ML-decision tree considers a dynamic sleep period range of 5 to 15 min to guarantee the operation.

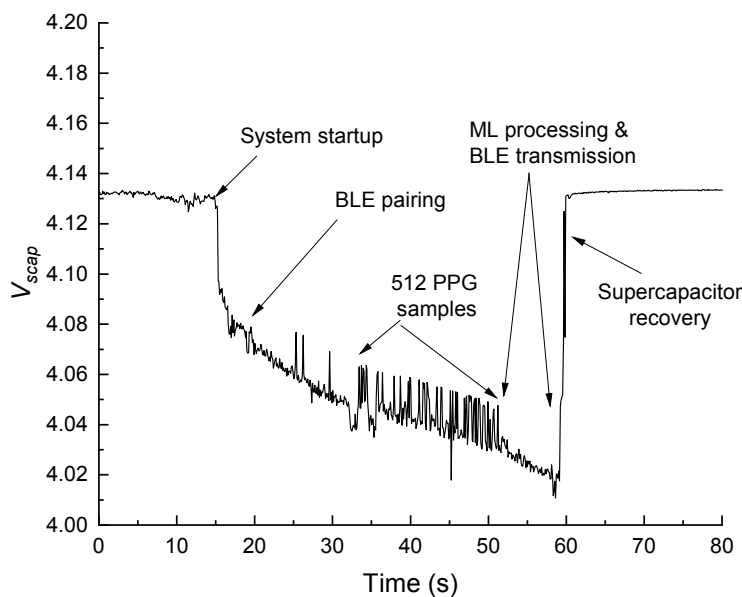


Figure 7. Measured supercapacitor voltage recovery after PPG sensing, processing, and BLE transmission.

Knowing the PPG sensing current consumption and their corresponding periods for each state, the prototype power consumption (mAh) is the following

$$Q = \frac{\Gamma}{\rho} \cdot (I_{PPG} T_{PPG} + I_{BLE} T_{BLE} + I_{Sleep} T_{Sleep} + I_{Proc} T_{Proc}), \quad (4)$$

where $I_{PPG} = 1.97$ mA is the sensor average current consumption with a data acquisition period of 20.4 s, I_{BLE} uses an average of 0.45 mA to send data packets in $T_{BLE} = 7.5$ s, $I_{Proc} = 0.42$ mA is the consumption during ML-decision tree processing in $T_{Proc} = 0.1$ s, and $I_{Sleep} = 34.3$ μ A is the average current consumption of the MCU in sleep mode for the sleep period T_{Sleep} . Moreover, T_{PPG} is configured at 25 Hz for the total of 512 measurements at 20.48 s. Here, Γ represents the number of sensing and transmission sequences during a day. If T_{sleep} is fixed ($\Gamma = 93.096$, $\rho = 3600$), the supercapacitor daily discharge is computed in $Q = 1.933$ mAh. This means that the entire IoWT system requires a total energy of 25.74 J per day to operate continuously, assuming a supercapacitor voltage of $V_{scap} = 3.7$ V.

The selected solar PV module has a value of $P_{MPPT} = 380.8$ mW at typical STC (i.e., 1000 W/m² and a cell temperature of 25 °C). Considering only 35% efficiency because the solar PV is being used as a wearable and assuming only five hours of irradiance at standard conditions (STC) [29], the energy generation is 99.72 J per day, which is 3.87 times the required energy of the system. Therefore, under the described conditions, the IoWT operation is guaranteed.

4.2. ML-Decision Tree Power Management Results

Decision trees are able to achieve high accuracy levels in ML-based classification-embedded implementations. However, it is necessary to carry out a training process carefully to avoid overfitting. In this sense, the training and validation process was generated by using a dataset of 1×10^7 samples according to the NEWS standard. From the dataset, 80% of data were used for the training process and 20% for the validation process.

For the experimental setup, three degrees of freedom are distinguished: (a) variations on PPG-based biosignal measurements (the Worst Case Scenario—WCS is with high variations because the system must decide between saving energy or sampling accurately), (b) supercapacitor's voltage level (low or high), and (c) the m -number of classes in the ML-DPMS, which corresponds to the sleep period in the MCU.

In this sense, two test case scenarios demonstrate the multimodal power management results based on the ML-decision tree approach.

- The first scenario considers biosignal measurements with medium to high SpO₂, Temp, and HR variations, with a critical behavior in samples 50 to 80 (See Figure 8a–c showing an SpO₂ level below 90%, Temperature of 40° and HR above 120). The supercapacitor voltage level, in Figure 8d, is above 4.0 V with a steady behavior at the beginning, and slow variations from sample 20. Five classes were employed in the experiment according to the following sleep periods: $m_1 = 5$ min, $m_2 = 7.5$ min, $m_3 = 10$ min, $m_4 = 12.5$ min and $m_5 = 15$ min.

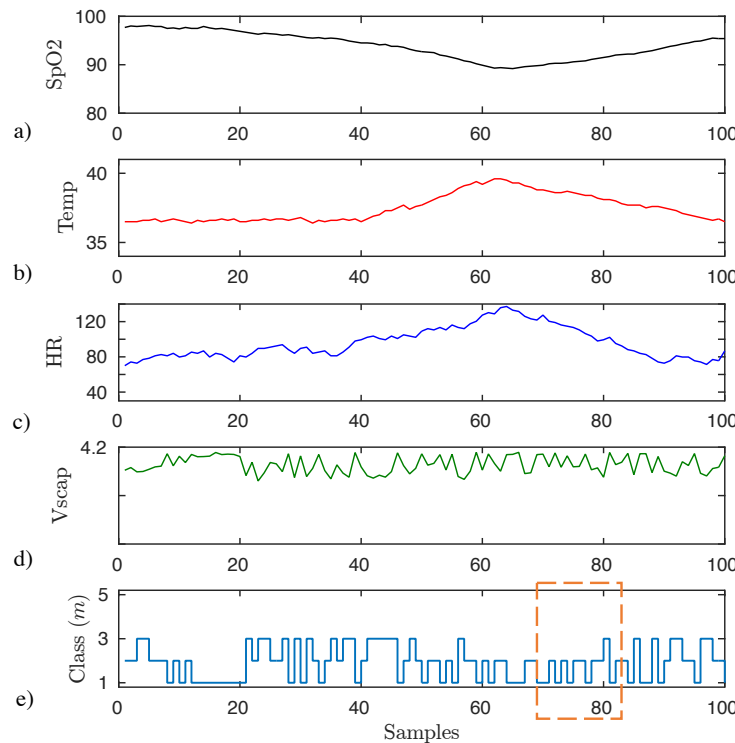


Figure 8. ML-decision tree results for test case scenario 1: (a–c) SpO₂, Temperature and Heart rate measurements; (d) Supercapacitor’s voltage; and (e) ML-decision tree classification results.

The ML-decision tree detects the quasi-stationary behavior of the supercapacitor and analyzes the biosignal variations, introducing shorter sleep periods than the traditional uniform power management. See Figure 8e with classification results from m_1 to m_3 in all the graphs, which means sleep period levels from 5 to 10 min. The results of test scenario 1 demonstrate the efficiency of the ML-decision tree power management. With sufficient energy in the supercapacitor and medium to high variations of the incoming data, the ML algorithm increases the sample period. Notice that during samples 50 to 80, the classification results were even shorter for $m_1 = 5$ min, and $m_2 = 7.5$ min.

Figure 9 highlights the red square region of the classification results of Figure 8e, i.e., the samples from 70 to 80. Here, a comparative analysis of the uniform power management strategy with our proposed ML-DPMS is presented. As one can notice, the ML-decision tree power management achieves 12 transmissions, 2.4× more than the uniform strategy with a sleep period of 15 min. In terms of energy consumption, the ML-DPMS approach requires 2.34 J and the uniform power management consumes 1.37 J. Therefore, one can see that multimodal power management has better energy use, with more transmissions when sensitive events are detected in the biosignal measurements, but with a relatively more energy consumption difference, i.e., 0.97 J, than the uniform strategy.

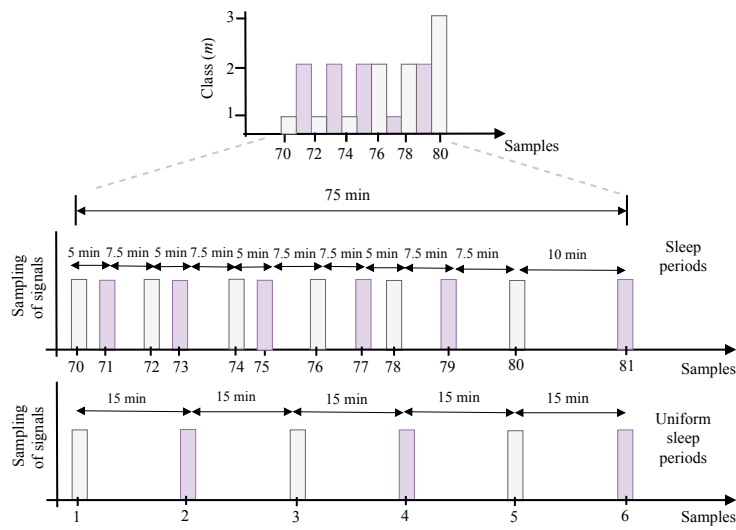


Figure 9. Comparative analysis result of ML-Decision tree and uniform power management for test scenario 1.

- The second test case scenario considers the same unstable behavior on the biosignal measurements as shown in Figure 10a–c. Five classes are also employed with the same range of test case 1.

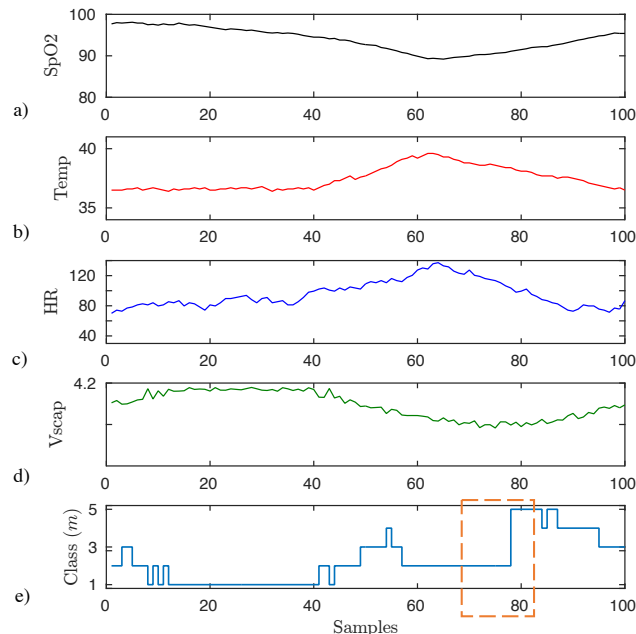


Figure 10. ML-decision tree results for test case scenario 2: (a–c) SpO₂, Temperature and Heart rate measurements; (d) Oscillatory supercapacitor's voltage; and (e) ML-decision tree classification results.

Although the unstable behavior of the biosignal measurements suggests shorter sample periods, the ML-decision tree analyzes the amount of energy stored in the supercapacitor (see the oscillatory behavior of V_{scap} in Figure 10d and the red square of Figure 10e).

The algorithm chooses the best sleep duty cycle, avoiding the system shutting down. The ML-decision tree algorithm also demonstrates a good balance between energy saving and accuracy. As one can notice from Figure 11 shows that the ML-DPMS prevents the system from shutting down by applying two large sleep periods in samples 79 and 80, resulting in an energy consumption of 1.53 J. This represents a 39.6% reduction in energy consumption compared to the uniform strategy's 2.52 J.

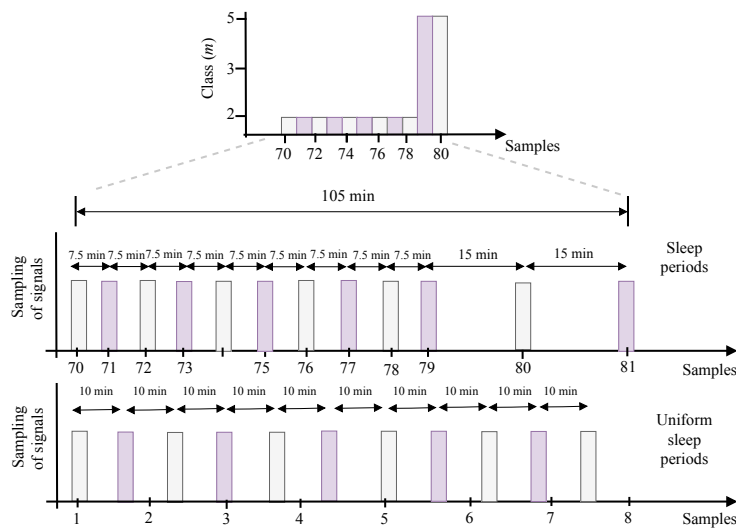


Figure 11. ML-decision tree and uniform power management comparative analysis for test scenario 2.

Considering the same samples marked on the square red of Figures 8 and 10, the results on both test cases demonstrate the smart and adaptive behavior of the decision tree-DPMS.

5. Discussion

A comparative analysis with other similar studies is presented in Table 1 to highlight the impact of the proposed ML-DPMS energy-saving technique for IoWT, which differs from previous studies [6,10,14,16,36]. In particular, [6,14] implement PPG signal analysis with intelligent processing, but without energy harvesting.

Table 1. Comparative analysis of the ML-DPMS approach.

	[6]	[10]	[14]	[36]	[16]	This Work
Management Technique	Threshold Decision	Temporal Convolutional Network	CNN + LSTM	LSTM + MLP	—	ML-Decision Tree + Dynamic PMS
Sensor	PPG	PPG	PPG	ECG	—	PPG
Wireless Protocol	Bluetooth	BLE	—	—	—	BLE
Storage Element	—	Li-Ion 370 mAh	—	—	—	Supercapacitor 8 F
Power Generation	—	—	—	—	900 μ W@ 272.7 μ A	99.72 J per day
Power Consumption	2.52 J	13.7 mW@ 4.5 mA	56.1 μ J per processed window	36.96 μ W	18 μ W@ 5.48 μ A	25.74 J per day
Energy Source	—	—	—	—	Kinetic microgenerators	Solar PV cell

In [10], a Q-PPG methodology based on a deep temporal convolutional network (TCN) was used to predict the user's heart rate (HR) using raw PPG and acceleration data in a low-cost, wireless wrist-worn device. The implementation also included intelligent processing, resulting in low power consumption. However, a one-to-one comparison cannot be made because the methodology was limited to real-time HR predictions and did not include the processing of a power management strategy. In fact, both strategies could be complementary in order to improve the power consumption performance. Likewise, Ref. [16] demonstrates lower power consumption than our study. However, this is due to the absence of a radio device, which is the component with the highest energy demand. The proposed multimodal power management aims to manage data interpretation and transmission following the IoWT paradigm.

The work in [36] also presents an algorithm for dynamic power management; however, it does not incorporate the multimodal approach for analyzing biosignal statistics and

supercapacitor energy availability. In contrast, our ML-DPMS algorithm is implemented in an embedded MCU device, enabling real-time decision-making and adaptation of the transmission duty cycle. Our experimental results demonstrate accurate operation for PPG biosignal measurements with high variability and supercapacitor voltage fluctuations which represents an attractive approach that other studies have not yet incorporated. Furthermore, the proposed prototype with multimodal power management achieves a total consumption of 25.74 J per day for uninterrupted operation.

On the other hand, other works have been proposed to provide solutions in the IoT field [37–42]. For example, Ref. [37] proposes a new hybrid power management strategy for use in wireless sensor networks, Ref. [38] proposes an AI-based IoT system with power management blocks. Moreover, a power management unit using solar energy harvesters for wireless sensor nodes is presented in [39]. Likewise, a strategy to achieve energy efficiency in wireless sensor networks can be found in [40]. Additionally, strategies for improving wireless sensor network performance can be seen in [41,42].

6. Conclusions

A novel multimodal power management strategy based on machine learning was proposed in this study. To evaluate its performance with real-time biosignal data, a wearable sensor node prototype was designed and constructed. The decision tree algorithm was implemented on the nRF52840 MCU and achieves a good balance between the saved energy and the duty cycle transmission. In the proposed test case scenarios, the ML-decision tree achieves at least $2.4\times$ more transmissions as well as avoids the system's power-off saving up to 39.6% of energy than the uniform power management. The energy analysis reveals a total consumption of 25.74 J per day to operate without interruption. Considering an efficiency of 35% for the flexible PV solar cell and only five hours of irradiance at standard conditions (STC) [29], the energy generation capacity was 99.72 J per day. This means that the system can generate 3.87 times more energy than what is required to operate without interruption.

Author Contributions: Conceptualization, A.C.-A., J.V.-C. and J.O.-A.; Formal analysis, A.C.-A., J.V.-C., E.O.-d.-l.-R., A.C.-A. and R.C.-A.; Investigation, A.C.-A., J.V.-C. and A.D.; Methodology, A.C.-A., J.V.-C., G.B.-N. and J.O.-A.; Project administration, J.V.-C. and J.O.-A.; Validation, G.B.-N., A.C.-A., E.O.-d.-l.-R., J.V.-C. and R.C.-A.; Writing original draft, A.C.-A., J.V.-C. and J.J.E.-L.; Writing review and editing, J.J.E.-L., J.V.-C., A.C.-A., R.C.-A. and A.D. All authors have read and agreed to the published version of the manuscript.

Funding: J. Ortegón-Aguilar, J. Vázquez-Castillo and A. Castillo-Atoche acknowledge the support of the Quintana Roo Science and Technology Council (COQCYT).

Institutional Review Board Statement: Not applicable.

Informed Consent Statement: Not applicable.

Data Availability Statement: Not applicable.

Conflicts of Interest: The authors declare no conflict of interest.

References

1. Xu, S.; Zhang, L.; Huang, W.; Wu, H.; Song, A. Deformable Convolutional Networks for Multimodal Human Activity Recognition Using Wearable Sensors. *IEEE Trans. Instrum. Meas.* **2022**, *71*, 1–14. [[CrossRef](#)]
2. Cheung, C.C.; Krahn, A.D.; Andrade, J.D. The Emerging Role of Wearable Technologies in Detection of Arrhythmia. *Can. J. Cardiol.* **2018**, *34*, 1083–1087. [[CrossRef](#)] [[PubMed](#)]
3. Jeong, I.C.; Bychkov, D.; Searson, P.C. Wearable Devices for Precision Medicine and Health State Monitoring. *IEEE Trans. Biomed. Eng.* **2019**, *66*, 1242–1258. [[CrossRef](#)]
4. Rando, E.; Pérez, P.; Scagliusi, S.F.; Medrano, F.J.; Huertas, G.; Yúfera, A. A Plethysmography Capacitive Sensor for Real-Time Monitoring of Volume Changes in Acute Heart Failure. *IEEE Trans. Instrum. Meas.* **2021**, *70*, 1–12. [[CrossRef](#)]
5. Meng, L.; Ge, K.; Song, Y.; Yang, D.; Lin, Z. Long-term Wearable Electrocardiogram Signal Monitoring and Analysis Based on Convolutional Neural Network. *IEEE Trans. Instrum. Meas.* **2021**, *70*, 1–11. [[CrossRef](#)]

6. Narendra Kumar Reddy, G.; Sabarimalai Manikandan, M.; Narasimha Murty, N.V.L. On-Device Integrated PPG Quality Assessment and Sensor Disconnection/Saturation Detection System for IoT Health Monitoring. *IEEE Trans. Instrum. Meas.* **2020**, *69*, 6351–6361. [[CrossRef](#)]
7. Starliper, N.; Mohammadzadeh, F.; Songkakul, T.; Hernandez, M.; Bozkurt, A.; Lobaton, E. Activity-Aware Wearable System for Power-Efficient Prediction of Physiological Responses. *Sensors* **2019**, *19*, 441. [[CrossRef](#)]
8. Oubre, B.; Daneault, J.F.; Boyer, K.; Kim, J.H.; Jasim, M.; Bonato, P.; Lee, S.I. A Simple Low-Cost Wearable Sensor for Long-Term Ambulatory Monitoring of Knee Joint Kinematics. *IEEE Trans. Biomed. Eng.* **2020**, *67*, 3483–3490. [[CrossRef](#)]
9. Lee, S.I.; Adans-Dester, C.P.; O'Brien, A.T.; Vergara-Diaz, G.P.; Black-Schaffer, R.; Zafonte, R.; Dy, J.G.; Bonato, P. Predicting and Monitoring Upper-Limb Rehabilitation Outcomes Using Clinical and Wearable Sensor Data in Brain Injury Survivors. *IEEE Trans. Biomed. Eng.* **2021**, *68*, 1871–1881. [[CrossRef](#)]
10. Burrello, A.; Pagliari, D.J.; Risso, M.; Benatti, S.; Macii, E.; Benini, L.; Poncino, M. Q-PPG: Energy-Efficient PPG-Based Heart Rate Monitoring on Wearable Devices. *IEEE Trans. Biomed. Circuits Syst.* **2021**, *15*, 1196–1209. [[CrossRef](#)]
11. Dell’Agnola, F.; Pale, U.; Marino, R.; Arza, A.; Atienza, D. MBioTracker: Multimodal Self-Aware Bio-Monitoring Wearable System for Online Workload Detection. *IEEE Trans. Biomed. Circuits Syst.* **2021**, *15*, 994–1007. [[CrossRef](#)] [[PubMed](#)]
12. Chaudhury, S.; Yu, C.; Liu, R.; Kumar, K.; Hornby, S.; Duplessis, C.; Sklar, J.M.; Epstein, J.E.; Reifman, J. Wearables Detect Malaria Early in a Controlled Human-Infection Study. *IEEE Trans. Biomed. Eng.* **2022**, *69*, 2119–2129. [[CrossRef](#)] [[PubMed](#)]
13. Davies, H.J.; Bachtiger, P.; Williams, I.; Molyneaux, P.L.; Peters, N.S.; Mandic, D.P. Wearable In-Ear PPG: Detailed Respiratory Variations Enable Classification of COPD. *IEEE Trans. Biomed. Eng.* **2022**, *69*, 2390–2400. [[CrossRef](#)] [[PubMed](#)]
14. Rocha, L.G.; Biswas, D.; Verhoef, B.E.; Bampi, S.; Van Hoof, C.; Konijnenburg, M.; Verhelst, M.; Van Helleputte, N. Binary CorNET: Accelerator for HR Estimation From Wrist-PPG. *IEEE Trans. Biomed. Circuits Syst.* **2020**, *14*, 715–726. [[CrossRef](#)] [[PubMed](#)]
15. Wang, N.; Zhou, J.; Dai, G.; Huang, J.; Xie, Y. Energy-Efficient Intelligent ECG Monitoring for Wearable Devices. *IEEE Trans. Biomed. Circuits Syst.* **2019**, *13*, 1112–1121. [[CrossRef](#)]
16. Mayer, P.; Magno, M.; Benini, L. Energy-Positive Activity Recognition - From Kinetic Energy Harvesting to Smart Self-Sustainable Wearable Devices. *IEEE Trans. Biomed. Circuits Syst.* **2021**, *15*, 926–937. [[CrossRef](#)]
17. Xu, C.; Song, Y.; Han, M.; Zhang, H. Portable and wearable self-powered systems based on emerging energy harvesting technology. *Microsystems Nanoeng.* **2021**, *7*, 3–14. [[CrossRef](#)]
18. Khalid, S.; Raouf, I.; Khan, A.; Kim, N.; Kim, H. A Review of Human-Powered Energy Harvesting for Smart Electronics: Recent Progress and Challenges. *Int. J. Precis. Eng. Manuf.-Green Tech.* **2019**, *6*, 821–851. [[CrossRef](#)]
19. Wei, Y.; Zhou, J.; Wang, Y.; Liu, Y.; Liu, Q.; Luo, J.; Wang, C.; Ren, F.; Huang, L. A Review of Algorithm and Hardware Design for AI-Based Biomedical Applications. *IEEE Trans. Biomed. Circuits Syst.* **2020**, *14*, 145–163. [[CrossRef](#)]
20. Qaim, W.B.; Ometov, A.; Molinaro, A.; Lener, I.; Campolo, C.; Lohan, E.S.; Nurmi, J. Towards Energy Efficiency in the Internet of Wearable Things: A Systematic Review. *IEEE Access* **2020**, *8*, 175412–175435. [[CrossRef](#)]
21. Wu, T.; Redouté, J.M.; Yuce, M.R. A Wireless Implantable Sensor Design With Subcutaneous Energy Harvesting for Long-Term IoT Healthcare Applications. *IEEE Access* **2018**, *6*, 35801–35808. [[CrossRef](#)]
22. Wang, W.; Xu, P.; Yang, L.T. Secure Data Collection, Storage and Access in Cloud-Assisted IoT. *IEEE Cloud Comput.* **2018**, *5*, 77–88. [[CrossRef](#)]
23. Savaglio, C.; Pace, P.; Aloisio, G.; Liotta, A.; Fortino, G. Lightweight Reinforcement Learning for Energy Efficient Communications in Wireless Sensor Networks. *IEEE Access* **2019**, *7*, 29355–29364. [[CrossRef](#)]
24. Golkarifard, M.; Yang, J.; Huang, Z.; Movaghari, A.; Hui, P. Dandelion: A Unified Code Offloading System for Wearable Computing. *IEEE Trans. Mob. Comput.* **2019**, *18*, 546–559. [[CrossRef](#)]
25. Fiandrino, C.; Allio, N.; Kliazovich, D.; Giaccone, P.; Bouvry, P. Profiling Performance of Application Partitioning for Wearable Devices in Mobile Cloud and Fog Computing. *IEEE Access* **2019**, *7*, 12156–12166. [[CrossRef](#)]
26. Lu, Y.; Ye, T.; Zheng, J. Decision Tree Algorithm in Machine Learning. In Proceedings of the 2022 IEEE International Conference on Advances in Electrical Engineering and Computer Applications (AEECA), Dalian, China, 20–21 August 2022; pp. 1014–1017. [[CrossRef](#)]
27. Fontaine, J.; Shahid, A.; Van Herbruggen, B.; De Poorter, E. Impact of Embedded Deep Learning Optimizations for Inference in Wireless IoT Use Cases. *IEEE Internet Things Mag.* **2022**, *5*, 86–91. [[CrossRef](#)]
28. Taghavi, M.; Shoaran, M. Hardware Complexity Analysis of Deep Neural Networks and Decision Tree Ensembles for Real-time Neural Data Classification. In Proceedings of the 2019 9th International IEEE/EMBS Conference on Neural Engineering (NER), San Francisco, CA, USA, 20–23 March 2019; pp. 407–410. [[CrossRef](#)]
29. Veligorskyi, O.; Khomenko, M.; Chakirov, R.; Vagapov, Y. Performance analysis of a wearable photovoltaic system. In Proceedings of the 2018 IEEE International Conference on Industrial Electronics for Sustainable Energy Systems (IESES), Hamilton, New Zealand, 31 January–2 February 2018; pp. 376–381. [[CrossRef](#)]
30. Nordic-Semiconductors. nRF52840 Dongle. 2020. Available online: <https://www.nordicsemi.com/Software-and-tools/Development-Kits/nRF52840-Dongle> (accessed on 1 July 2020).
31. Maxim Integrated: PPG Algorithms Specifications. Available online: <https://www.maximintegrated.com/en/design/technical-documents/app-notes/7/7272.html> (accessed on 29 July 2022).
32. Béres, S.; Hejjel, L. The minimal sampling frequency of the photoplethysmogram for accurate pulse rate variability parameters in healthy volunteers. *Biomed. Signal Process. Control.* **2021**, *68*, 102589. [[CrossRef](#)]

33. Baek, H.; Shin, J.; Jin, G. Reliability of the Parabola Approximation Method in Heart Rate Variability Analysis Using Low-Sampling-Rate Photoplethysmography. *J. Med. Syst.* **2017**, *41*, 189. [[CrossRef](#)]
34. Elgendi, M.; Fletcher, R.; Liang, Y. The use of photoplethysmography for assessing hypertension. *NPJ Digit. Med.* **2019**, *2*, 60. [[CrossRef](#)]
35. NEWS: National Early Warning Score. Available online: <https://www.rcplondon.ac.uk/projects/outputs/national-early-warning-score-news-2> (accessed on 5 August 2022).
36. Sivapalan, G.; Nundy, K.K.; Dev, S.; Cardiff, B.; John, D. ANNet: A Lightweight Neural Network for ECG Anomaly Detection in IoT Edge Sensors. *IEEE Trans. Biomed. Circuits Syst.* **2022**, *16*, 24–35. [[CrossRef](#)]
37. Chéour, R.; Jmal, M.W.; Khriji, S.; El Houssaini, D.; Trigona, C.; Abid, M.; Kanoun, O. Towards Hybrid Energy-Efficient Power Management in Wireless Sensor Networks. *Sensors* **2021**, *22*, 301. [[CrossRef](#)] [[PubMed](#)]
38. Shyam Sunder Reddy, K.; Manohara, M.; Shailaja, K.; Revathy, P.; Kumar, T.M.; Premalatha, G. Power management using AI-based IOT systems. *Meas. Sens.* **2022**, *24*, 100551. [[CrossRef](#)]
39. Lopez-Gasso, A.; Beriain, A.; Solar, H.; Berenguer, R. Power Management Unit for Solar Energy Harvester Assisted Batteryless Wireless Sensor Node. *Sensors* **2022**, *22*, 7908. [[CrossRef](#)] [[PubMed](#)]
40. Barati, A.; Movaghar, A.; Sabaei, M. Energy Efficient and High Speed Error Control Scheme for Real Time Wireless Sensor Networks. *Int. J. Distrib. Sens. Netw.* **2014**, *10*, 698125. [[CrossRef](#)]
41. Barati, A.; Movaghar, A.; Sabaei, M. RDTP: Reliable Data Transport Protocol in Wireless Sensor Networks. *Telecommun. Syst.* **2016**, *62*, 611–623. [[CrossRef](#)]
42. Khazaei, E.; Barati, A.; Movaghar, A. Improvement of fault detection in wireless sensor networks. In Proceedings of the 2009 ISECS International Colloquium on Computing, Communication, Control, and Management, Sanya, China, 8–9 August 2009; Volume 4, pp. 644–646. [[CrossRef](#)]

Disclaimer/Publisher's Note: The statements, opinions and data contained in all publications are solely those of the individual author(s) and contributor(s) and not of MDPI and/or the editor(s). MDPI and/or the editor(s) disclaim responsibility for any injury to people or property resulting from any ideas, methods, instructions or products referred to in the content.